2023-09

Using Sentinel-1 data for soybean harvest detection in Vojvodina province, Serbia

Marković Miljana, Živaljević Branislav, Mimić Gordan, Woznicki Sean, Marko Oskar, Lugonja Predrag

Using Sentinel-1 data for soybean harvest detection in Vojvodina province, Serbia

Miljana Marković[a], Branislav Živaljević[a], Gordan Mimić[a], Sean Woznicki[b], Oskar Marko[a], and Predrag Lugonja[a]

[a]University of Novi Sad, BioSense Institute, Dr. Zorana Djindjića 1, Novi Sad, Serbia
[b]Grand Valley State University, Robert B. Annis Water Resources Institute, 740 West Shoreline Dr, Muskegon, Michigan, United States

ABSTRACT

Information on crop harvest events has become valuable input for models related to food security and agricultural management and optimization. Precise large scale harvest detection depends on temporal resolution and satellite images availability. Synthetic Aperture Radar (SAR) data are more suitable than optical, since the images are not affected by clouds. This study compares two methods for harvest detection of soybean in Vojvodina province (Serbia), using the C-band of Sentinel-1. The first method represents a maximum difference of ascending VH polarization backscatter (σ_{VH}) between consecutive dates of observation. The second method uses a Radar Vegetation Index (RVI) threshold value of 0.39, optimized to minimize Mean Absolute Error (MAE). The training data consisted of 50 m point buffers' mean value with ground-truth harvest dates (n=100) from the 2018 and 2019 growing seasons. The first method showed better performance with Pearson correlation coefficient r=0.85 and MAE=5 days, whereas the calculated metrics for the RVI threshold method were r=0.69 and MAE=8 days. Therefore, validation was performed only for the method of maximum VH backscatter difference where mean values of parcels with ground-truth harvest dates for 2020 had generated the validation dataset (n=67). Performance metrics (r=0.83 and MAE=3 days) confirmed the suitability for accurate harvest detection. Ultimately, a soybean harvest map was generated on a parcel level for Vojvodina province.

Keywords: Sentinel-1, harvest detection, soybean, SAR data, VH polarization

1. INTRODUCTION

Soybean (*Glycine max L.*) is one of the world's most important agricultural crops whose grain is used as a source of edible oil (18-24%) and protein (35-50%) in human and livestock nutrition and for industrial purposes.[1] Since the beginning of the 1970s, when the Landsat program was launched, the application of remote sensing in agriculture has advanced significantly and has become an important tool for planning agricultural production, with the aim of increasing yields while reducing investment costs.[2] Remotely sensed data can provide accurate and timely information about the development of vegetation and the phenological stage of a certain crop.[3] Further, information regarding when and where crops are harvested can provide valuable insight into the amount of food that will be available on the market.

In the optimization of crop harvesting practices, remote sensing is a useful method since satellite images provide a large spatial coverage in short time intervals of days to weeks. With the launch of the Sentinel satellites (Sentinel-1 and Sentinel-2) in 2016, the ability to detect the optimal harvest date has increased significantly.[4]

Optical satellite images can provide good information on crop growth and development, but their analysis is limited to cloud-free conditions, which significantly affects information availability, spatial and temporal resolution.[5] Compared to optical imaging, SAR (Synthetic Aperture Radar) has certain characteristics that can be significant for crop condition monitoring. Firstly, the microwave frequencies it uses can penetrate through clouds, which allows uninterrupted observations at certain time intervals.[6] In addition, SAR is sensitive to biomass geometry,

Further author information: (Send correspondence to Miljana Marković & Branislav Živaljević)
Miljana Marković: E-mail: miljana.markovic@biosense.rs
Branislav Živaljević: E-mail: branislav.zivaljevic@biosense.rs

Remote Sensing for Agriculture, Ecosystems, and Hydrology XXV, edited by Christopher M. U. Neale, Antonino Maltese, Proc. of SPIE Vol. 12727, 127271G · © 2023 SPIE · 0277-786X · doi: 10.1117/12.2679417

thus can potentially detect changes in crop height before and after harvest.[7] Scenes can include one or two out of four polarization bands based on instrument settings: single-band VV or HH, and dual-band VV+VH or HH+HV, where each band corresponds to specific polarizations such as vertical or horizontal transmit and receive.[6]

Both sensors are found to be sensitive to crop harvest events, albeit in different ways. Optical data is more sensitive to the change of the biophysical status of the crop on the ground, while SAR can provide insights about the crops' structural change. Some studies point out that the coherence and the VV/VH backscatter ratio of Sentinel-1 can be particularly sensitive to crop harvest events.[8–10] In this case study, remote sensing techniques were used for the detection of soybean harvest dates over large areas as well as on the parcel level. In the last couple of years several research studies were conducted on this particular subject.

Different machine learning techniques gave results using Sentinel-1 imagery and applying interferometric coherence with a final mean absolute error of 6 days (MAE = 6).[11] The most frequently analyzed crops are soybeans, maize and sunflower, but also sugarcane in parts of Southeast Asia and Australia, for which there are tested methods combining Sentinel-1 and Sentinel-2 images, with an achieved precision of 4 days.[12,13] However, this field of research is still in its beginning stages and there is much progress to be done in perspective.

With each new Sentinel-1 image, these maps could potentially be used for monitoring the occurrence and frequency of allergic reactions to ragweed in different areas of Vojvodina Province, since this weed often grows on soybean fields.[14] By harvesting the entire field, the dispersal of allergenic particles is greater than usual, therefore the maps of recently harvested soybean fields are of great interest for future analysis and precautionary measures in Vojvodina Province.[15]

The aim of this research was to detect soybean harvest dates, as one of the most cultivated agricultural crops in the Vojvodina Province, in the northern part of Serbia. This study compares two methods for harvest detection of soybean in Vojvodina province (Serbia), using the C-band of Sentinel-1. The first method uses a Radar Vegetation Index (RVI) threshold approach, while the second one uses a maximum difference of ascending VH polarization backscatter (σ_{VH}) between consecutive dates of observation. The time series of Sentinel-1 images was analyzed to observe the behavioral rules of soybean crop phenology during the period of vegetative maturation for three seasons (2018-2020). The highest precision was achieved by observing the maximum difference of ascending VH polarization of consecutive Sentinel-1 images.

2. MATERIALS AND METHODS

2.1 Study area

The Vojvodina Province is the northern part of the Republic of Serbia (Figure 1), with a total area of 2.150.000 ha, and is located on the southern edge of the Pannonian Plain.[16] The area is characterized by a moderately warm climate, with hot summers and cold winters. Most precipitation occurs in the form of rain during the spring-summer transition period (May-June).[17] The average annual temperature is 11.1°C, while the average amount of precipitation is 606 mm.[18] Vojvodina Province is characterized by predominantly agricultural land (83%), most of which is cropland (77%), with intensive agriculture[19] and soybean as one of the most cultivated crops, according to the Statistical Office of the Republic of Serbia.[20–22]

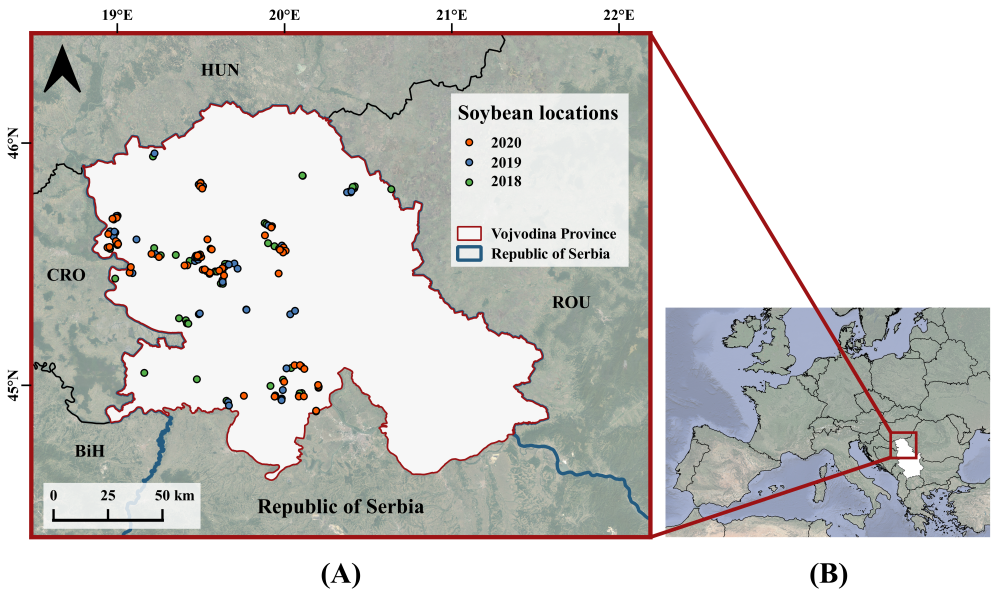

Figure 1. Spatial distribution of points in study area (A) and the location of the study area in Southeastern Europe (B)

2.2 Data

The data needed for this research was received from the agricultural company, and was obtained as points (latitude and longitude) representing one parcel. Therefore, each point represents one pixel and holds information on location, together with the date of sowing and harvesting for a period of 3 years, i.e. from 2018 to 2020. Figure 1 shows the locations of the points during each year in the study area. To provide relevant representations of each parcel, buffers of 50 meters were created around each point and used in further analysis. However, after visual inspection of Sentinel-2 RGB images, some of the buffers were overlapping boundaries to neighboring crops due to small parcels or the location of points near the border. Those buffers were excluded from further analysis, resulting in the number of final buffers for 2018 being 83, 66 in 2019, and 88 in 2020.

C-band SAR data were extracted from the Google Earth Engine platform, which contains Sentinel-1 Ground Range Detected (GRD) scenes, calibrated and ortho-corrected images by using the Sentinel-1 Toolbox. Prior to downloading the data, Focal Mean[23] speckle filter was applied to limit the noise within a 30-meter radius circle. The VV and VH polarizations from both ascending and descending orbit were acquired for each buffer and backscatter coefficients (σ_{VV}, σ_{VH}) time-series were generated for each year. The time series was established using the first and final harvest dates obtained from the initial ground truth data, covering 20th August to 20th October. Although the temporal resolution is 6 days, for some locations there is information every 1-3 days due to overlapping scenes.

Two methods were applied:

1. Radar Vegetation Index - **RVI Threshold Method**
2. Maximum difference of backscatter polarization - **Maximum Difference Method**

For both methods data from 2018 and 2019 were used for training and 2020 for testing. The performances of the methods were assessed using the following metrics: Pearson's correlation coefficient (r), coefficient of determination (R^2), Mean Absolute Error (MAE), and Root Mean Square Error (RMSE).

2.3 Radar Vegetation Index

The Radar Vegetation Index (RVI) is a vegetation index considered suitable for monitoring vegetation by utilizing information obtained from radar signals.[24] RVI value ranges between 0 and 1 and is a measure of volume scattering, mathematically represented with Equation 1.

$$RVI = \frac{8\sigma_{\mathrm{HV}}}{\sigma_{\mathrm{HH}} + \sigma_{\mathrm{VV}} + 2\sigma_{\mathrm{HV}}}, \tag{1}$$

Where σ_{HH}, σ_{HV} and σ_{VV} represent the measured linear backscattering intensities. Due to the absence of HH and HV backscattering coefficients in the dataset, we substituted them with VV and VH backscatter coefficients, following the approach suggested by Nasirzadehdizaji[25] and Charbonneau.[26] Thus, the final formulation of RVI is given in Equation 2:

$$RVI = \frac{4\sigma_{\mathrm{VH}}}{\sigma_{\mathrm{VV}} + \sigma_{\mathrm{VH}}}, \tag{2}$$

Given its frequent utilization as a vegetation index derived from Synthetic Aperture Radar (SAR) data for vegetation growth[27–30] and its correlation with the Normalized Difference Vegetation Index (NDVI),[31,32] we investigated its utility for harvest detection. The range of RVI values from 0.3 to 0.45 was tested to determine the optimal threshold for identifying the harvesting by minimizing MAE in days. Among the evaluated RVI values, 0.39 emerged as the threshold that resulted in the lowest MAE and was selected as the final threshold for harvest determination. An example of an RVI time series for a specific buffer point, along with its corresponding harvest date, is illustrated in Figure 2.

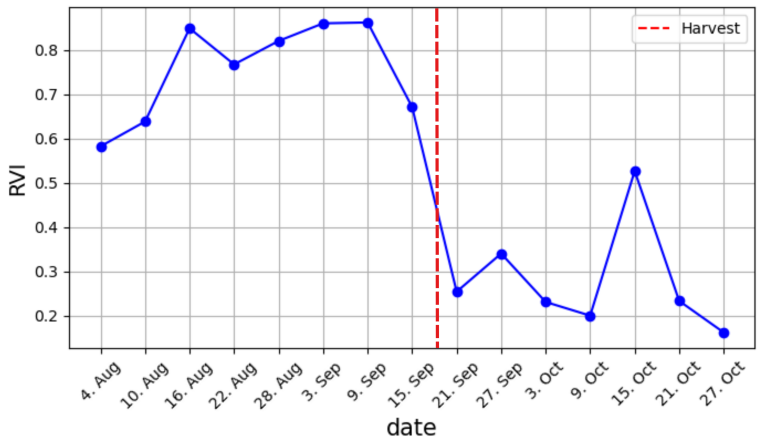

Figure 2. An example of a Radar Vegetation Index (RVI) time series for one point for the period August-October

2.4 Maximum difference

Analyzing the time series of ascending and descending VH and VV polarizations, a significant drop of signal occurs immediately after harvesting for ascending σ_{VH} polarization. For that purpose, the difference between consecutive dates of observation was calculated. Considering that backscatter polarization is in negative decibels and that time series was differentiated, the minimum negative value was an indicator of harvesting. In other words, it represented the maximum negative difference between the dates. Further in text, the term 'maximum difference' will be used for simplicity, referring to the 'maximum negative difference'. Due to the possibility of multiple high signal oscillations, we analyzed the three largest signal drops (Figure 3) as potential harvesting events, while defining the value that occurred first in time as the actual harvest. The harvest date was determined as the mean date between two dates corresponding to the maximum difference.

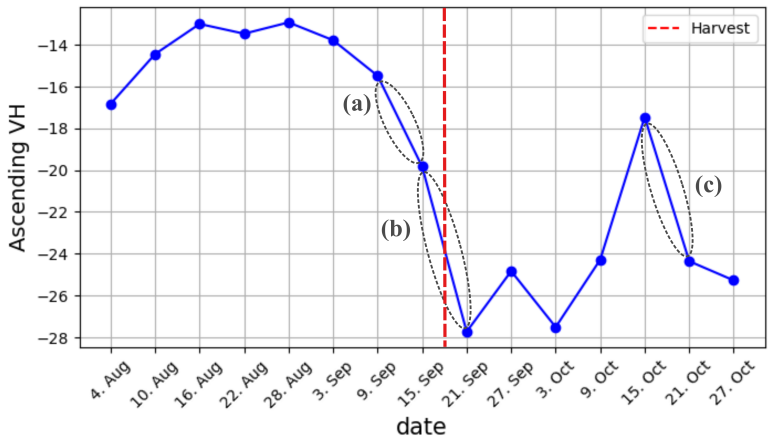

Figure 3. An example of ascending VH polarization time series for one point for the period August-October

3. RESULTS AND DISCUSSION

3.1 RVI Threshold Method

The RVI Threshold Method was applied to the data from the years 2018 and 2019, identifying the first RVI value below 0.39 as the indicator for the onset of harvest period. Pearson's r between the ground truth data and the predicted values was 0.69, indicating a moderate positive relationship. Furthermore, the algorithm's performance was assessed using the MAE and RMSE, which were found to be 8 and 11 days (Figure 4), respectively, signifying the level of accuracy and prediction errors in the model.

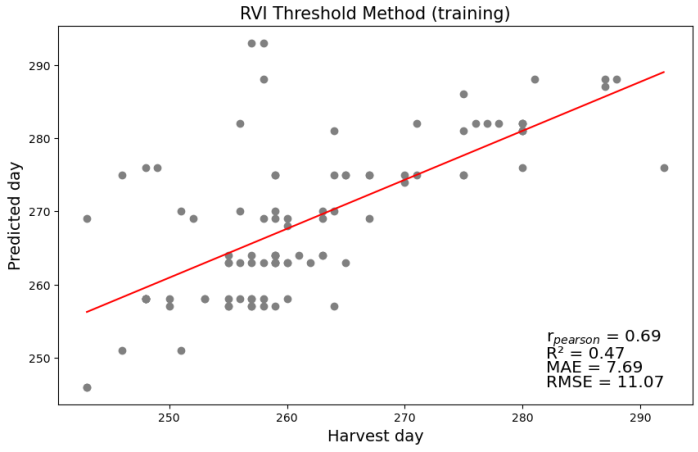

Figure 4. Scatter plot of training data using the RVI Threshold Method

3.2 Maximum Difference Method

The Maximum Difference Method encompassed a training phase, during which correlations were analyzed using data from the years 2018 and 2019. Three distinct cases were analyzed, namely, the one (Figure 3, (b)), two (Figure 3, (b and c)) and three (Figure 3, (a, b and c)) largest signal drops. For the scenarios involving the two and three signal drops, the algorithm was designed to prioritize the value that occurred earliest in time and declare it as the predicted harvest date. Pearson's correlations were 0.91, 0.85, and 0.66, respectively (Figure 5). As well, MAE values were 3, 5, and 8 days, while RMSE values were 5, 7, and 11 days for the same datasets.

These results indicate the most effectiveness of the one and two signal drops, while the analysis of three drops was excluded from the further steps.

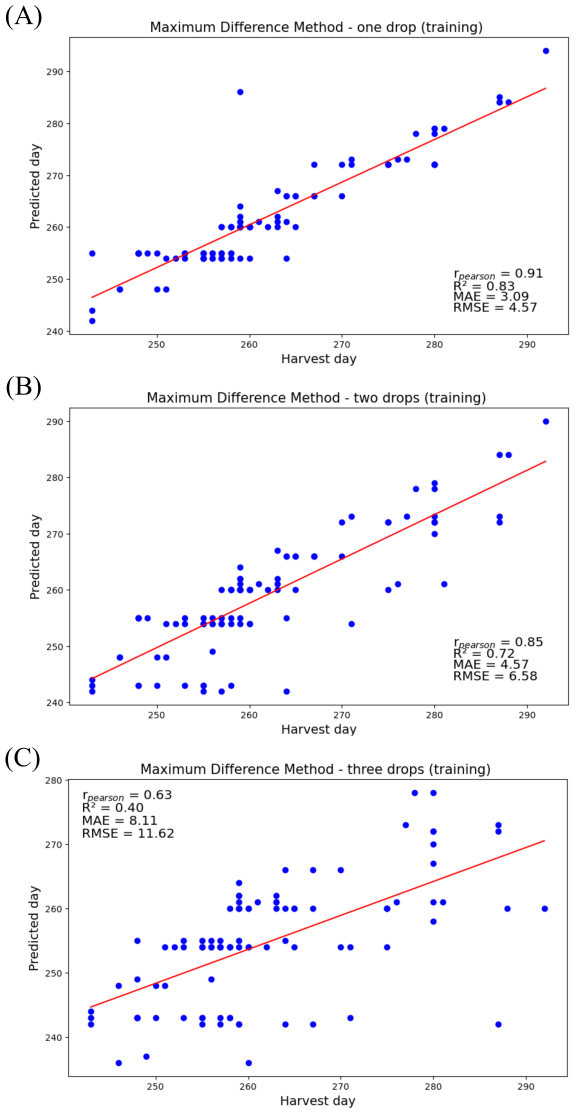

Figure 5. Scatter plot of training data using Maximum Difference Method with (A) one, (B) two and (c) three signal drops

Next step was to test the results using data from the year 2020. The testing process involved generating a parcel-level map of predicted harvest days. Firstly, a soybean parcel-level map was created through the utilization of cadastral parcels and soybean classification for the corresponding year. A classification map was provided by BioSense Institute which classifies main crops every year using the Random Forest algorithm with Sentinel-2 and ground truth data.[33,34] After creating a soybean parcel-level map, the σ_{VH} backscatter time-series polarization was extracted for each parcel and the same algorithm was used as in the case of the buffer training data. Identified harvest days were assigned to corresponding parcels, creating a harvest map (Figure 7). The testing procedure showed significantly better metrics when using the two signal drops (Figure 6).

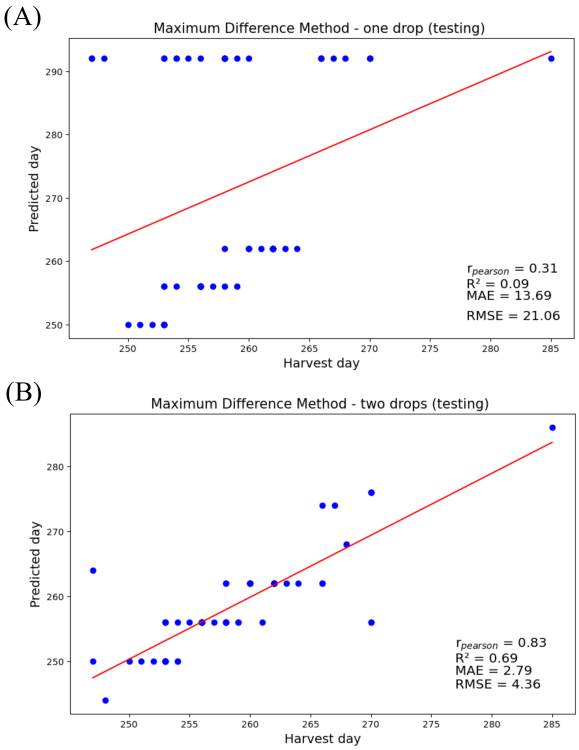

Figure 6. Scatter plot of testing data using Maximum Difference Method with (A) one, (B) two signal drops

Pearson's r of 0.83 and MAE of 3 days indicate very good accuracy, therefore, this method was selected as the final approach for detecting harvest dates, enabling accurate timely detection. Figure 7 illustrates the harvest map for 2020 generated by applying this method.

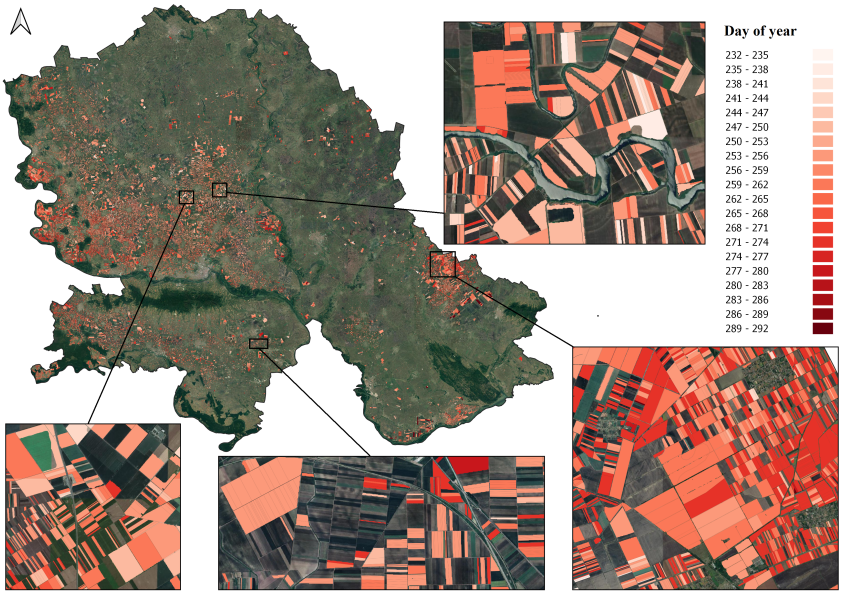

Figure 7. Soybean harvest map for 2020 created by Maximum Difference Method with two signal drops

3.3 Discussion

According to our knowledge, the analysis of RVI behavior has not been the subject of previous studies for harvest detection, despite being researched in various crop monitoring and classification studies. Therefore, this paper presents a novel examination of RVI with a revealed threshold of 0.39 and achieved 8 days precision for soybean harvest detection.

However, regarding the Maximum Difference Method, Stasolla and Neyt[12] came to similar conclusions for sugarcane by analyzing the VH polarization and observing a significant drop in signal response after harvest. Compared to their 4-day detection accuracy results, our research showed that for soybean, it is possible to accomplish 3-day precision with a modified methodology of considering the two largest drops in σ_{VH} and using only the ascending orbit.

Kavats[35] and Amherdt[11] also detected the soybean harvest using radar images. However, they used VV polarization and interferometric coherences, achieving a precision of 6 days. The precision of 3 days for soybean harvest detection was also achieved by Shendryk,[13] who combined the threshold method with the use of Sentinel-2 data and climate parameters in the final classification. This finding further validates the usefulness of our proposed method, which offers a significantly simpler and faster algorithm with the same precision.

The final maps, created by the proposed method, can only be generated at the end of the entire harvest season. These maps find application in yield prediction, optimization, and plot management logistics. However, future advancements will involve the development of real-time harvest identification methods, during the harvest season. Additionally, efforts will be made to extend these methods to other crops as well.

4. CONCLUSIONS

In this study, we compared two methods for detecting soybean harvest. Firstly, we investigated the behavior of the Radar Vegetation Index for harvest detection and focused on defining a suitable threshold and possible precision.

Secondly, we explored the second approach based on the observation of VH polarization values. We found that the ascending VH polarization values significantly decreased after the harvest event. Utilizing this information, we identified two distinct drops and, based on our analysis, declared the earliest drop as the soybean harvest event. This method is demonstrated as a reliable one for soybean harvest detection with accuracy of ± 3 days. The outcomes of this research highlighted the applicability and reliability of the Maximum Difference Method to detect soybean harvest effectively.

This study demonstrates the potential of remote sensing techniques, especially SAR data, for agricultural purposes. As well, it contributes valuable insights into soybean harvest detection, clearing the path for improving resource management and agricultural optimization, as the demand for sustainable and efficient agriculture continues to grow.

ACKNOWLEDGMENTS

This research is part of the ANTARES project that has received funding from the European Union's Horizon 2020 research and innovation programme under the European Union's Horizon 2020 research and innovation programme (SGA-CSA. No. 739570 under FPA No. 664387).We also extend our gratitude to Delta Agrar for providing us with the necessary data.

REFERENCES

[1] Pratap, A., Gupta, S. K., Kumar, J., and Solanki, R., "Soybean," *Technological Innovations in Major World Oil Crops, Volume 1: Breeding* , 293–321 (2012).

[2] Atzberger, C., "Advances in remote sensing of agriculture: Context description, existing operational monitoring systems and major information needs," *Remote sensing* **5**(2), 949–981 (2013).

[3] Tuszynska, J., Gatkowska, M., Wrobel, K., and Jagiello, K., "A pilot study on determining approximate date of crop harvest on the basis of sentinel-2 satellite imagery," *Geoinformation Issues* **10**(1 (10)) (2018).

[4] Bégué, A., Arvor, D., Bellon, B., Betbeder, J., De Abelleyra, D., PD Ferraz, R., Lebourgeois, V., Lelong, C., Simões, M., and R. Verón, S., "Remote sensing and cropping practices: A review," *Remote Sensing* **10**(1), 99 (2018).

[5] Cheng, Y., Vrieling, A., Fava, F., Meroni, M., Marshall, M., and Gachoki, S., "Phenology of short vegetation cycles in a kenyan rangeland from planetscope and sentinel-2," *Remote sensing of environment* **248**, 112004 (2020).

[6] "Sentinel-1 sar user handbook." Accessed: July 18, 2023.

[7] Nasirzadehdizaji, R., Cakir, Z., Sanli, F. B., Abdikan, S., Pepe, A., and Calo, F., "Sentinel-1 interferometric coherence and backscattering analysis for crop monitoring," *Computers and Electronics in Agriculture* **185**, 106118 (2021).

[8] Veloso, A., Mermoz, S., Bouvet, A., Le Toan, T., Planells, M., Dejoux, J.-F., and Ceschia, E., "Understanding the temporal behavior of crops using sentinel-1 and sentinel-2-like data for agricultural applications," *Remote sensing of environment* **199**, 415–426 (2017).

[9] Khabbazan, S., Vermunt, P., Steele-Dunne, S., Ratering Arntz, L., Marinetti, C., van der Valk, D., Iannini, L., Molijn, R., Westerdijk, K., and van der Sande, C., "Crop monitoring using sentinel-1 data: A case study from the netherlands," *Remote Sensing* **11**(16), 1887 (2019).

[10] Bonte, K., Moshtaghi, M., Van Tricht, K., and Tits, L., "Automated crop harvest detection algorithm based on synergistic use of optical and radar satellite imagery," in [*2021 IEEE International Geoscience and Remote Sensing Symposium IGARSS*], 5981–5984, IEEE (2021).

[11] Amherdt, S., Di Leo, N. C., Balbarani, S., Pereira, A., Cornero, C., and Pacino, M. C., "Exploiting sentinel-1 data time-series for crop classification and harvest date detection," *International Journal of Remote Sensing* **42**(19), 7313–7331 (2021).

[12] Stasolla, M. and Neyt, X., "Applying sentinel-1 time series analysis to sugarcane harvest detection," in [*IGARSS 2019-2019 IEEE International Geoscience and Remote Sensing Symposium*], 1594–1597, IEEE (2019).

[13] Shendryk, Y., Pan, L., Craigie, M., Stasolla, M., Ticehurst, C., and Thorburn, P., "A satellite-based methodology for harvest date detection and yield prediction in sugarcane," in [*IGARSS 2020-2020 IEEE International Geoscience and Remote Sensing Symposium*], 5167–5170, IEEE (2020).

[14] Barnes, E. R., Jhala, A. J., Knezevic, S. Z., Sikkema, P. H., and Lindquist, J. L., "Soybean and common ragweed (ambrosia artemisiifolia) growth in monoculture and mixture," *Weed technology* **33**(3), 481–489 (2019).

[15] Smith, M., Cecchi, L., Skjøth, C., Karrer, G., and Šikoparija, B., "Common ragweed: a threat to environmental health in europe," *Environment international* **61**, 115–126 (2013).

[16] Košćal, M., Menković, L., Mijatović, M., and Knežević, M., "Geomorfološka karta autonomne pokrajine vojvodine 1: 200 000," (2005).

[17] Beck, H. E., Zimmermann, N. E., McVicar, T. R., Vergopolan, N., Berg, A., and Wood, E. F., "Present and future köppen-geiger climate classification maps at 1-km resolution," *Scientific data* **5**(1), 1–12 (2018).

[18] Hrnjak, I., Lukić, T., Gavrilov, M. B., Marković, S. B., Unkašević, M., and Tošić, I., "Aridity in vojvodina, serbia," *Theoretical and applied climatology* **115**, 323–332 (2014).

[19] Ćirić, V., Drešković, N., Mihailović, D., Mimić, G., Arsenić, I., and urević, V., "Which is the response of soils in the vojvodina region (serbia) to climate change using regional climate simulations under the sres-a1b?," *Catena* **158**, 171–183 (2017).

[20] [*Statistical Office of the Republic of Serbia*], Statistical Office of the Republic of Serbia (2018).

[21] [*Statistical Office of the Republic of Serbia*], Statistical Office of the Republic of Serbia (2019).

[22] [*Statistical Office of the Republic of Serbia*], Statistical Office of the Republic of Serbia (2020).

[23] Gorelick, N., Hancher, M., Dixon, M., Ilyushchenko, S., Thau, D., and Moore, R., "Google earth engine: Planetary-scale geospatial analysis for everyone," *Remote sensing of Environment* **202**, 18–27 (2017).

[24] Kim, Y. and van Zyl, J., "On the relationship between polarimetric parameters," in [*IGARSS 2000. IEEE 2000 International Geoscience and Remote Sensing Symposium. Taking the Pulse of the Planet: The Role of Remote Sensing in Managing the Environment. Proceedings (Cat. No. 00CH37120)*], **3**, 1298–1300, IEEE (2000).

[25] Nasirzadehdizaji, R., Balik Sanli, F., Abdikan, S., Cakir, Z., Sekertekin, A., and Ustuner, M., "Sensitivity analysis of multi-temporal sentinel-1 sar parameters to crop height and canopy coverage," *Applied Sciences* **9**(4), 655 (2019).

[26] Charbonneau, F., Trudel, M., and Fernandes, R., "Use of dual polarization and multi-incidence sar for soil permeability mapping," in [*Proceedings of the 2005 advanced synthetic aperture radar (ASAR) workshop, St-Hubert, QC, Canada*], 15–17 (2005).

[27] Xie, Q., Lai, K., Wang, J., Lopez-Sanchez, J. M., Shang, J., Liao, C., Zhu, J., Fu, H., and Peng, X., "Crop monitoring and classification using polarimetric radarsat-2 time-series data across growing season: A case study in southwestern ontario, canada," *Remote Sensing* **13**(7), 1394 (2021).

[28] Mandal, D., Kumar, V., Ratha, D., Dey, S., Bhattacharya, A., Lopez-Sanchez, J. M., McNairn, H., and Rao, Y. S., "Dual polarimetric radar vegetation index for crop growth monitoring using sentinel-1 sar data," *Remote Sensing of Environment* **247**, 111954 (2020).

[29] Mandal, D., Ratha, D., Bhattacharya, A., Kumar, V., McNairn, H., Rao, Y. S., and Frery, A. C., "A radar vegetation index for crop monitoring using compact polarimetric sar data," *IEEE Transactions on Geoscience and Remote Sensing* **58**(9), 6321–6335 (2020).

[30] Ratha, D., Mandal, D., Kumar, V., McNairn, H., Bhattacharya, A., and Frery, A. C., "A generalized volume scattering model-based vegetation index from polarimetric sar data," *IEEE Geoscience and Remote Sensing Letters* **16**(11), 1791–1795 (2019).

[31] Gonenc, A., Ozerdem, M. S., and Emrullah, A., "Comparison of ndvi and rvi vegetation indices using satellite images," in [*2019 8th International Conference on Agro-Geoinformatics (Agro-Geoinformatics)*], 1–4, IEEE (2019).

[32] Kumar, D., Rao, S., and Sharma, J., "Radar vegetation index as an alternative to ndvi for monitoring of soyabean and cotton," in [*Proceedings of the XXXIII INCA International Congress (Indian Cartographer), Jodhpur, India*], 19–21 (2013).

[33] Lugonja, P., Brdar, S., Simović, I., Mimić, G., Palamarchuk, Y., Sofiev, M., and Šikoparija, B., "Integration of in situ and satellite data for top-down mapping of ambrosia infection level," *Remote Sensing of Environment* **235**, 111455 (2019).

[34] Crnojević, V., Lugonja, P., Brkljač, B., and Brunet, B., "Classification of small agricultural fields using combined landsat-8 and rapideye imagery: case study of northern serbia," *Journal of Applied Remote Sensing* **8**(1), 083512–083512 (2014).

[35] Kavats, O., Khramov, D., Sergieieva, K., and Vasyliev, V., "Monitoring harvesting by time series of sentinel-1 sar data," *Remote Sensing* **11**(21), 2496 (2019).